Eur Biophys J (2008) 37:421–433
DOI 10.1007/s00249-007-0227-2

ORIGINAL PAPER

Effect of divalent cations on the structure of the antibiotic daptomycin

Steven W. Ho · David Jung · Jennifer R. Calhoun · James D. Lear · Mark Okon · Walter R. P. Scott · Robert E. W. Hancock · Suzana K. Straus

Received: 13 August 2007 / Revised: 2 October 2007 / Accepted: 9 October 2007 / Published online: 30 October 2007

Abstract Daptomycin, a cyclic anionic lipopeptide antibiotic, whose three-dimensional structure was recently solved using solution state NMR (Ball et al. 2004; Jung et al. 2004; Rotondi and Gierasch 2005), requires calcium for function. To date, the exact nature of the interaction between divalent cations, such as Ca^{2+} or Mg^{2+}, has not been fully characterized. It has, however, been suggested that addition of Ca^{2+} to daptomycin in a 1:1 molar ratio induces aggregation. Moreover, it has been suggested that certain residues, e.g. Asp3 and Asp7, which are essential for activity (Grunewald et al. 2004; Kopp et al. 2006), may also be important for Ca^{2+} binding (Jung et al. 2004). In this work, we have tried: (1) to further pinpoint how Ca^{2+} affects daptomycin structure/oligomerization using analytical ultracentrifugation; and (2) to determine whether a specific calcium binding site exists, based on one-dimensional ^{13}C NMR spectra and molecular dynamics (MD) simulations. The centrifugation results indicated that daptomycin formed micelles of between 14 and 16 monomers in the presence of a 1:1 molar ratio of Ca^{2+} and daptomycin. The ^{13}C NMR data indicated that addition of calcium had a significant effect on the Trp1 and Kyn13 residues, indicating that either calcium binds in this region or that these residues may be important for oligomerization. Finally, the molecular dynamics simulation results indicated that the conformational change of daptomycin upon calcium binding might not be as significant as originally proposed. Similar studies on the divalent cation Mg^{2+} are also presented. The implication of these results for the biological function of daptomycin is discussed.

Keywords Daptomycin · Ca^{2+} binding · Mg^{2+} binding · analytical ultracentrifugation · molecular dynamics (MD) simulation · NMR · Nuclear overhauser enhancement (NOE)

Steven W. Ho and David Jung have contributed equally to this work.

Electronic supplementary material The online version of this article (doi:10.1007/s00249-007-0227-2) contains Supplemental Material, which is available to authorized users.

S. W. Ho · M. Okon · W. R. P. Scott · S. K. Straus (✉)
Department of Chemistry, University of British Columbia, 2036 Main Mall, Vancouver, BC, Canada V6T 1Z1
e-mail: sstraus@chem.ubc.ca

D. Jung · R. E. W. Hancock
Department of Microbiology and Immunology, University of British Columbia, 232B-2259 Lower Mall, Vancouver, BC, Canada V6T 1Z4

J. R. Calhoun · J. D. Lear
Department of Biochemistry and Biophysics, University of Pennsylvania, School of Medicine, 422 Curie Boulevard, Philadelphia, PA 19104-6059, USA

Introduction

Daptomycin, currently sold under the tradename Cubicin, is a novel antibiotic, recently approved by the US FDA to target Gram-positive pathogens. It is a cyclic anionic tridecapeptide, with a number of D-amino acids (D-asparagine, D-alanine, and D-serine), three uncommon amino acid residues (ornithine, (2S,3R)-3-methyl-glutamic acid and kynurenine), and a N-terminus that is acylated with a *n*-decanoyl fatty acid side chain. It has been found to be an effective antimicrobial agent against methicillin-resistant *Staphylococcus aureus*, as well as vancomycin resistant Enterococci, penicillin-resistant Streptococci, and coagulase-negative Staphylococci (Eliopoulos et al. 1986; Fass

and Helsel 1986; Jones and Barry 1987; Streit et al. 2005; Tally and DeBruin 2000).

A number of studies have shown that daptomycin displays antimicrobial activity only in the presence of calcium (Boaretti et al. 1993; Laganas et al. 2003; Lakey et al. 1989; Lakey and Ptak 1988; Silverman et al. 2001, 2003). Two mechanisms have been proposed for the mode of action of this antimicrobial peptide: (1) daptomycin inhibits lipoteichoic acid biosynthesis in the presence of calcium ions (Boaretti et al. 1993), although this has been disputed (Silverman et al. 2003); and (2) daptomycin binds calcium, followed by a change in its conformation (Jung et al. 2004), which allows the peptide to insert more deeply into the membrane bilayer. This in turn leads to membrane depolarization and results in cell death (Jung et al. 2004; Silverman et al. 2001, 2003).

In order to better understand the role of calcium in the function of daptomycin and to understand structure:function relationships, Ball et al. (2004), Jung et al. (2004) and Rotondi and Gierasch (2005) independently determined the structure of the peptide in the absence of calcium, using solution state NMR. All three studies resulted in different structures for the apo-form being proposed. The backbone Cα RMSDs between the 1T5M consensus structure (Jung et al. 2004), solved using a 2 mM daptomycin solution in 100 mM KCl, 0.2 mM EDTA, 5 mM $CaCl_2$, pH 6.70, and 1XT7 (Ball et al. 2004), eludicated using a 1.2 mM solution of daptomycin in 90% H_2O/10% D_2O, are large (3.2 Å). A comparison of the 1T5M consensus structure and the Rotondi and Gierasch structures (backbone Cα RMSDs > 4 Å, for the family of 6 structures that emerged from their RMSD analysis (Rotondi and Gierasch 2005)) show that the differences are even larger in this case. In the latter case, the sample was prepared by adding daptomycin in small portions to a sample buffer, consisting of 10 mM sodium phosphate, pH 5.3, 10% D_2O in H_2O (v/v), which was degassed using multiple cycles of the freeze–vacuum–thaw method, such that the final concentration of daptomycin was 1.9 mM. The conformational heterogeneity is even larger if the lipid tail and side chains are taken into account. In addition to the apo-form, Jung et al. (2004) determined the structure of the peptide in the presence of calcium and demonstrated that the binding of Ca^{2+} causes a conformational change of daptomycin based on the presence of additional NOE cross-peaks in the NOESY spectrum. In other words, a change from an ill-defined conformation (in the apo-form) to a well-defined one was suggested upon addition of calcium. This change in structure was not observed by Ball et al. (2004). Rotondi and Gierasch (2005) report that under the sample conditions used to minimize aggregation, a well-defined conformation was observed only in the calcium-free form. All three studies did find that the presence of calcium leads to line broadening caused by aggregation of daptomycin. Titration experiments revealed that the ^1H linewidths of all residues increase with increasing calcium concentration up to one molar equivalent (Ball et al. 2004), suggesting a one to one stoichiometric ratio of calcium to daptomycin.

Given the structural changes observed by NMR and data obtained from circular dichroism, fluorescence experiments, and functional assays (e.g. calcein leakage), Jung et al. (2004) proposed a new mechanism for the mode of action of the lipopeptide, namely one in which calcium triggers two structural transitions in two steps. The first binding event of Ca^{2+} in solution serves to enhance the amphipathicity of daptomycin leading to insertion into the membrane, in addition to acting as a bridge for inducing oligomerization of daptomycin. Interestingly, Rotondi and Gierasch suggest that daptomycin is also amphipathic in an aqueous environment. Inspection of the structure of daptomycin obtained by Ball et al. (2004) led them to suggest that the four acidic residues, Asp3, Asp7, Asp9 and MeGlu12 (in the apo structure) are not close enough to render an effective Ca^{2+} binding site. In contrast, Jung et al. (2004) hypothesized that the first calcium binding site may be located between Asp3 and Asp7. The structure of tsushimycin (Bunkoczi et al. 2005), a lipopeptide antibiotic, recently solved by X-ray crystallography to 1.0 Å resolution, supported this suggestion, as the Ca^{2+} ion was found to be located between Asp1 and Asp5 in this cyclic peptide.

The second conformational change requires both calcium and negatively charged liposomes, in particular a 1:1 ratio of 1-palmitoyl-2-oleoyl-*sn*-glycero-3-phosphocholine (POPC) and 1-palmitoyl-2-oleoyl-*sn*-glycero-3-phospho-*rac*-1-glycerol (POPG). This second conformational change has not been characterized structurally. Recent evidence based on fluorescence measurements and FRET studies suggested that this step also involves aggregation and daptomycin requires Ca^{2+} in order to perturb model bacterial membranes consisting of POPC/POPG (1:1).

Recently, Grunewald et al. (2004) have performed a series of derivitization experiments on daptomycin and measured bioactivities of these modified peptides by determining the minimum inhibitory concentration (MIC) in the presence of calcium. Their results indicate that the methyl-group in MeGlu12 is crucial for activity, as well as the residue Kyn13. To probe the role of acidic residues and calcium in antimicrobial activity, they also replaced each acidic sidechain in daptomycin in turn (Asp to Asn, Glu to Gln) and determined the MIC. The acidic sidechains of Asp3 and MeGlu12 were found not to be important for bactericidal potency, whereas mutation of Asp7 and Asp9 individually led to a total loss of bioactivity.

In this contribution, we seek to further characterize the effect of the divalent cations Ca^{2+} and Mg^{2+} on the

structure and aggregation state of daptomycin in the absence of lipids. The binding of calcium and magnesium was probed using analytical ultracentrifugation. We also report the structure of a 2.5:1 Mg^{2+}/daptomycin complex obtained using ^{1}H two-dimensional NMR spectroscopy, along with activity (minimal inhibitory concentration, MIC) data. In addition, one-dimensional ^{13}C calcium titration NMR experiments were used to determine which residues are most affected by the presence of calcium and/or the formation of aggregates. Finally, time-averaged NMR refinement (Torda and van Gunsteren 1991) with molecular dynamics simulations was used to postulate the nature of the structure of calcium-bound aggregated daptomycin, and to determine whether a specific cation-binding site exists. While the 1T5N structure was refined using NOEs determined from Ca^{2+}-bound daptomycin, no Ca^{2+} was explicitly present in the refinement procedure. Here, we formulated five different hypotheses of how calcium might be bound to daptomycin and then tested each by assessing to what extent these models agree with the NOE data.

Methods

Analytical ultracentrifugation experiments

A 2.5 mM daptomycin solution (daptomycin was provided by Cubist Pharmaceuticals) was prepared by dissolving 23.2 mg of peptide stock in 5.8 ml of 100 mM KCl, pH 7.0. A stock solution of $CaCl_2$ was made such that the concentration was 2 M, pH 7.0. Samples were prepared by adding the following equivalents of metal to peptide: 0.25 (or 0.625 mM), 0.5 (1.25 mM), 0.75 (1.875 mM), 1 (2.5 mM), and 2.5 (6.25 mM). The samples were allowed to equilibrate at room temperature overnight prior to being placed in the centrifuge. Similarly, a stock solution of $MgCl_2$ (2 M, pH 7.0) was prepared and added to the peptide solution such that similar equivalents of metal to peptide were added as for the calcium case.

Measurements were made using a Beckman XLI analytical ultracentrifuge. Sedimentation equilibrium experiments were done at 40, 45, and 50 KRPM in six-channel, carbon-epoxy composite centerpieces supplied by Beckman. Equilibrium was assessed by the absence of significant change in radial concentration gradients (measured using interference optics) in scans separated by a few hours. Data were analyzed by curve fitting to an equation describing the sedimentation equilibrium for a monomer and independent (not in equilibrium exchange) *n*-mer aggregate using Igor-Pro® (Wavemetrics, Lake Oswego OR). The equation is

$$S(r) = S_1(r_o)\exp\left\{\frac{(1-\bar{v}\rho)\omega^2 M_n}{2RT}\left(r^2 - r_o^2\right)\right\} + S_2(r_o)\exp\left\{\frac{(1-\bar{v}\rho)\omega^2 n M_n}{2RT}\left(r^2 - r_o^2\right)\right\}$$

where:

$S_1(r_o)$	signal from monomeric species at radial position r_o from the center of rotation.
$S_2(r_o)$	signal at r_o from n-mer aggregate of monomers
$\bar{v}$	partial specific volume of sedimenting species (cc/g)
ρ	density of supporting buffer (g/cc)
ω	angular velocity of rotor (radians/s)
M_n	molecular weight of monomeric species (g/mole)
R	gas constant (8.315×10^7 ergs K^{-1} mol^{-1})
T	temperature (K)

The peptide partial specific volume (0.668) was estimated by curve fitting of the data taken in the absence of Ca^{2+} or Mg^{2+} and assuming the peptide to be monomeric (as judged by the small observed concentration gradients). Using this value, data at different Ca^{2+} or Mg^{2+} concentrations were fitted, and the relative contributions of monomer and *n*-mer species determined by integrating their individual signal profiles over the volume of the cell. Fits using aggregation numbers between 12 and 17 were compared using the sums of squared residuals.

Minimal inhibitory concentration (MIC)

The minimal inhibitory concentration of daptomycin was determined using the microtitre broth dilution method (Amsterdam 1996). Briefly, an overnight culture of *S. aureus* (ATCC 25923) grown in Mueller Hinton Broth at 37°C was diluted to 10^5 and added to a 100 µl well of a 96 well polypropylene plate (Corning, Whitby, ON). The wells contained 2 mM of the desired divalent cation ($CaCl_2$, $MnCl_2$, $MgCl_2$, $CuCl_2$, and $NiCl_2$). A serial dilution of daptomycin ranging between 64 and 0.125 µg/ml was used. The 96 well plate was incubated overnight at 37°C and the MIC was determined at the concentration of daptomycin at which all bacterial growth was inhibited.

NMR spectroscopy and structure calculations

The Mg^{2+}-conjugated NMR sample contained 2 mM daptomycin, 100 mM KCl, 5 mM $MgCl_2$, and 7% D_2O (Cambridge Isotopes, Andover, MA). All NMR spectra collected at 35°C were recorded using a Varian Inova800

located at the Environmental Molecular Sciences Laboratory in the Pacific Northwest National Laboratory. Spectra collected at 18°C were recorded on a Varian Unity500 spectrometer operated by the UBC Laboratory for Molecular Biophysics. Homonuclear TOCSY (spin lock time = 60 ms) (Braunschweiler and Ernst 1983), NOESY (τ_m = 150 ms) (Jeener et al. 1979), and DQF-COSY (Rance et al. 1983) were collected at 18°C and at 35°C.

All NMR spectra for the magnesium containing daptomycin sample were processed with NMRPipe (Delaglio et al. 1995) and analyzed using NMRVIEW v.5.0.4 (Johnson and Blevins 1994). Conversion of NOE volumes to distance restraints and pseudoatom corrections were calculated as previously described (Rozek et al. 2000). Structure calculations were performed using the DGII module of Insight II v.97.2 (Accelrys Inc., San Diego, CA). Calculated structures were accepted based on the lowest NOE distance restraint violations and best convergence. The structures were further analyzed using MOLMOL v.2K.1 (Koradi et al. 1996).

Calcium titration by ^{13}C NMR

The initial sample for the calcium titration was prepared as described in Jung et al. (2004). It contained 2.5 mM daptomycin, 100 mM KCl, 0.2 mM EDTA and 7% D_20 (Cambridge Isotopes, Andover, MA). A solution of 1 M $CaCl_2$ was added in 2 µl aliquots, corresponding to a 0.5 mM Ca^{2+} concentration increase for each step. In other words, eight samples containing 0–3.5 mM Ca^{2+} relative to 2.5 mM daptomycin were prepared. In terms of molar ratios, this corresponds to calcium to daptomycin ratios ranging from 0:1 to 1.4:1, in steps of 0.2. The pH of the starting solution was adjusted to 6.6 and measured at the end of the titration to verify if it remained constant, which it did.

All one-dimensional ^{13}C NMR spectra collected at 25°C were recorded on a Varian Unity 500 using a standard pulse sequence. The spectra were all processed with the same phase correction and a linebroadening of 10 Hz. The peak positions and linewidths (full width at half height) were determined by fitting each resonance to a Lorentzian, using the program DMFIT (Massiot et al. 2002). The one-dimensional spectra were referenced to the methyl group of external 2,2-dimethyl-2-silapentane-5-sulfonic acid (DSS). Assignments of the carbons were made using two-dimensional HMBC, HMQC, and HSQC data (data not shown) and the ^1H assignments reported in Jung et al. (2004). The latter spectra were recorded on a Varian 600 MHz instrument at 25°C, using a calcium-free sample, as described above.

Molecular dynamics simulations

All simulations were performed using the GROMOS96 (Scott et al. 1999; van Gunsteren et al. 1996) biomolecular simulation package and the 43A1 force field (van Gunsteren et al. 1996). The different models investigated were solvated in explicit SPC water (Berendsen et al. 1981). Truncated octahedron periodic boundary conditions were imposed. Simulations were performed in the NPT ensemble (T = 300 K, P = 1 atm) using the Berendsen weak coupling methods (Berendsen et al. 1984). Covalent bonds were constrained using the SHAKE method (Ryckaert et al. 1977), with a relative geometric tolerance of 10^{-4}. A reaction field (Tironi et al. 1995) long-range correction to the truncated Coulomb potential was applied. All simulations were performed for 30 ns after equilibration. See Supplemental Material for a detailed description of the refinement protocol and analysis tools applied.

The calcium binding sites, which were tested, are summarized in Table 1. For each type of binding site probed, a particular NMR structure from the ensemble of 17 calcium bound structures in PDB entry 1T5N (Jung et al. 2004) was selected as is indicated in Table 1. Only in one case, for structure #13 in Table 1, were the side-chains of Asp3 and Asp7 rotated to create a better binding site between the calcium and oxygens of the sidechains.

Results

Aggregation state of daptomycin in the presence of Ca^{2+} or Mg^{2+}

In order to quantify the aggregation state of daptomycin upon addition of calcium and magnesium, analytical ultracentrifugation experiments were performed. For calcium, it was found that addition of up to 0.75 equivalents had little effect on oligomerization, but once a 1:1 ratio of calcium to daptomycin was reached, multimers formed. The data at different Ca^{2+} concentrations were fitted and the relative contributions of monomer and n-mer species were determined by integrating their individual signal profiles over the volume of the cell, as described in the "Methods". Fits using aggregation numbers between 12 and 17 were compared using the sums of squared residuals (Fig. 1a). An aggregation number of 14 was chosen for weight fraction comparisons because it was the lower limit of range (14–16) giving visually identical fits to the data. Data points and fit lines for 0.5, 0.75, and 1.0 equivalents of Ca^{2+} at all three speeds are shown in Fig. 1b. The weight fraction of 14-mer is shown in Fig. 1c. This suggested that at a 1:1 calcium to daptomycin ratio, a micellar structure forms. This was consistent with the ^1H (Ball et al. 2004;

Table 1 Calcium binding sites probed by molecular dynamic simulations

Model	Calcium bound between	Experimental evidence from reference	Structure number from 1T5N
i	Asp3 and Asp7 sidechains	(Bunkoczi et al. 2005; Jung et al. 2004)	6, 7, and 13
ii	Asp3 sidechain and Thr4/Orn6 backbone	(Chattopadhyaya et al. 1992; Chazin 1995; Marsden et al. 1990)	1 and 5
iii	Asp7 sidechain and Ala8 backbone	(Chattopadhyaya et al. 1992; Chazin 1995; Marsden et al. 1990)	9
iv	MeGlu12 sidechain and backbone and Kyn13 backbone	this work	6
v	Asp7 and Asp9 sidechains	(Grunewald et al. 2004)	2 and 17
vi			all

For each model the calcium-oxygen bond lengths were set to 2.5 Å. Calcium-bound (1T5N) structures from Jung et al. (2004) were used to construct the models (see text)

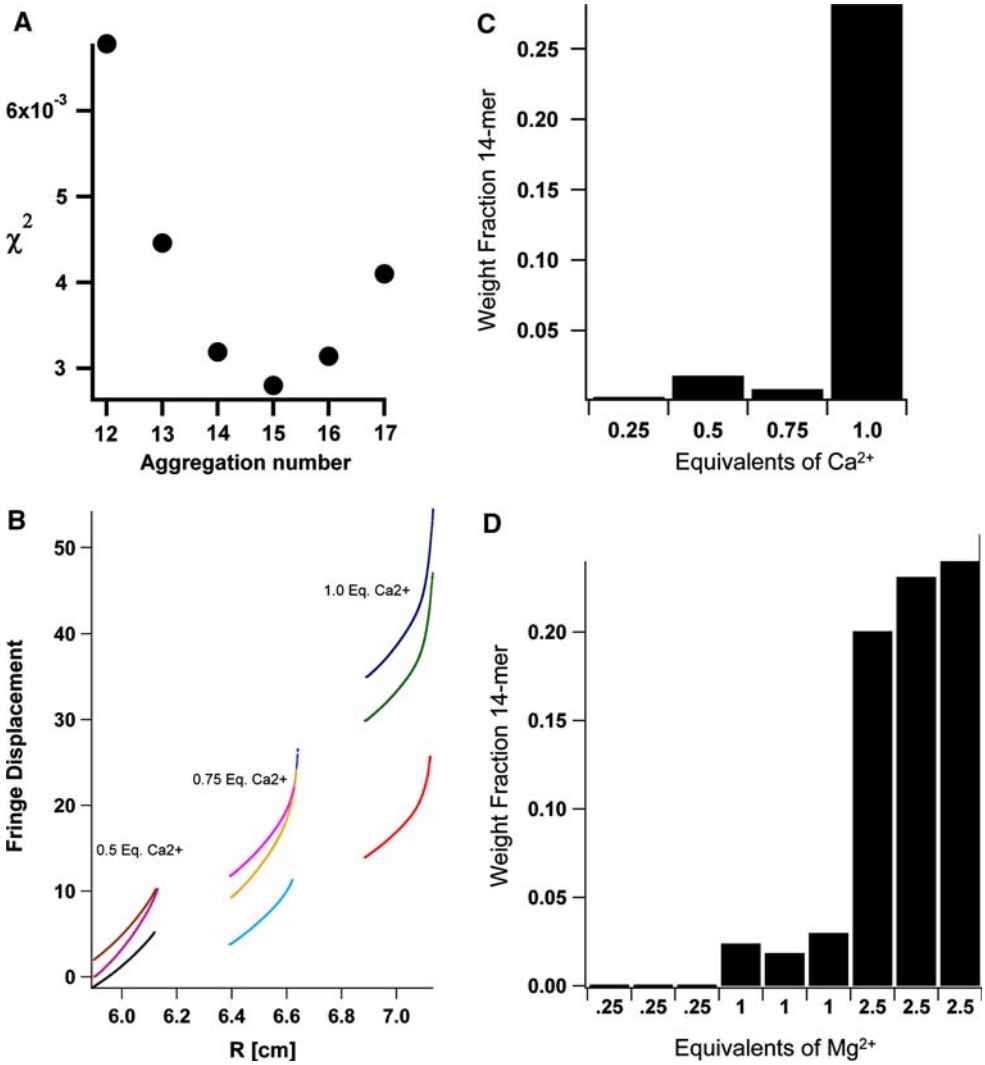

Fig. 1 **a** Sums of squared residuals obtained for equilibrium sedimentation experiments performed on daptomycin with increasing calcium concentration. Aggregation numbers between 12 and 17. **b** Fit lines found for the fringe displacement as a function of cell coordinate for 0.5, 0.75, and 1.0 equivalents of Ca^{2+} at all three speeds. The color scheme is arbitrary. **c** Weight fraction of 14-mer in the presence of Ca^{2+}. An aggregation number of 14 was chosen because it was the lower limit of the range (14–16) giving visually identical fits to the data (as seen in **a**). **d** Weight fraction of 14-mer in the presence of Mg^{2+}. An aggregation number of 14 was chosen because it was the lower limit of the range (14–16) giving visually identical fits to the data (not shown)

Jung et al. 2004; Rotondi and Gierasch 2005) and ^{13}C NMR data (*vide infra*). For magnesium ion, 2.5 equivalents of Mg^{2+} were needed to promote micelle formation (Fig. 1d).

Daptomycin activity and structure in the presence of Mg^{2+}

To quantify the effect of magnesium on daptomycin activity and structure, we determined the MIC of daptomycin with a range of divalent cations that included Ca^{2+}, Mn^{2+}, Mg^{2+}, Cu^{2+}, and Ni^{2+}. The results indicated that substituting calcium with any of these divalent cations caused a minimum 32-fold increase in the MIC (Table 2). This factor increased further to >100-fold, when MICs were determined using depleted Mueller Hinton Broths (Ca^{2+} concentration = 0 mM) (J. Silverman, personal communication).

To see if the increase in MIC with the calcium substitutes was correlated with changes in the structural characteristics of daptomycin, we determined the three-dimensional structure of daptomycin in the presence of 2.5 equivalents of Mg^{2+} and compared the Mg^{2+}-substituted daptomycin structure to the apo and Ca^{2+}-conjugated structures of daptomycin that were previously determined (Jung et al. 2004). Chemical shift assignments of the Mg^{2+}-substituted daptomycin were obtained using standard NMR methods (Wüthrich 1986). Spectra were initially collected at 35°C in order to compare the spectra of the Mg^{2+}-substituted sample with the spectra that were used to calculate the Ca^{2+}-conjugated structure. The NOESY spectrum of the Mg^{2+}-substituted sample at 35°C (τ_m = 150 ms) was fairly well resolved and showed no line broadening. The spectrum showed no resemblance to the Ca^{2+}-conjugated structure that had extensive line broadening. Instead, the Mg^{2+}-substituted NOESY spectrum at 35°C resembled more closely the NOESY spectrum of apo-daptomycin. Spectra of the Mg^{2+}-substituted sample were therefore collected at 18°C (τ_m = 150 ms) in order to compare these spectra with the apo-daptomycin spectra that we previously collected at 17°C (τ_m = 150 ms). Like the apo NOESY spectrum, the Mg^{2+}-substituted NOESY spectrum (Fig. 2a) showed no extensive line-broadening. There were no NOE contacts between the *n*-decanoyl fatty acid chain with any of the side chains, which we previously saw in the NOESY spectrum of the Ca^{2+}-conjugated spectrum. There was also no difference in the chemical shift between the Mg^{2+} and apo samples. NOE-based distance restraints for the Mg^{2+}-substituted sample were collected from the 18°C NOESY spectrum. An overview of the NOE restraints used to calculate the proposed three-dimensional structures of daptomycin in the presence of Mg^{2+} is shown in Fig. 2b, and a statistical summary of the structure calculation is given in Table 3.

A total of 62 NOE restraints were identified and used for the structure calculation. Out of the 62 identified NOE restraints, there were no medium or long range NOE distance restraints. The overall backbone RMSD of the Mg^{2+}-substituted structure was lower then the apo-daptomycin structure, which suggests that the Mg^{2+}-substituted structure was more well defined, especially around Ala 8, as compared to the apo structure. However, there were no major structural differences between the Mg^{2+}-substituted structure and the apo-daptomycin structure (Fig. 3). Therefore, the binding of Mg^{2+} to daptomycin did not cause any significant structural rearrangements in daptomycin.

Table 2 Minimal inhibitory concentration values of *S. aureus* treated with daptomycin and 2 mM $CaCl_2$, 2 mM $MnCl_2$, 2 mM $MgCl_2$, 2 mM $CuCl_2$, and 2 mM $NiCl_2$

$CaCl_2$	1 μg/ml
$MnCl_2$	32 μg/ml
$MgCl_2$	>64 μg/ml
$CuCl_2$	>64 μg/ml
$NiCl_2$	>64 μg/ml

Ca^{2+}-bound structure of daptomycin

Given that the oligomerization state of daptomycin was not known at the time when the 1T5N structure of the 1:1 Ca^{2+}/daptomycin complex was solved, we reexamined this structure in detail. Firstly, we carried out extensive NOE refinement molecular dynamics simulations to, on the one hand, determine how well the Ca^{2+}-bound structural models agreed with the experimental ^1H NMR data (Jung et al. 2004) when an explicit Ca^{2+} binding site is taken into account, and on the other, to determine whether a preferential binding site could be found. Out of the 17 total configurations obtained from the NMR data of calcium-bound daptomycin (PDB entry 1T5N, refined without calcium) (Jung et al. 2004), only the conformations that would best suit the hypothesized mode of calcium binding were used as starting coordinates for each of the five groups of models (Table 1). In the first set of models (i), calcium was located in between Asp3 and Asp7. The next set of groups (ii and iii) were postulates based on existing knowledge of other well-studied calcium binding proteins in which calcium is analogously positioned in the most negatively charged region of the protein, such as e.g. calmodulin and annexin IV. Group iv incorporated the results from the NMR titration experiment reported here, and finally, group v incorporated the experimental evidence from Grunewald et al. (2004) that Asp7 and Asp9 are absolutely essential for the biological activity of daptomycin (Kopp et al. 2006). Finally, the 17 NMR derived Ca^{2+}-bound conformations from Jung et al. (2004) (group vi) were included in the

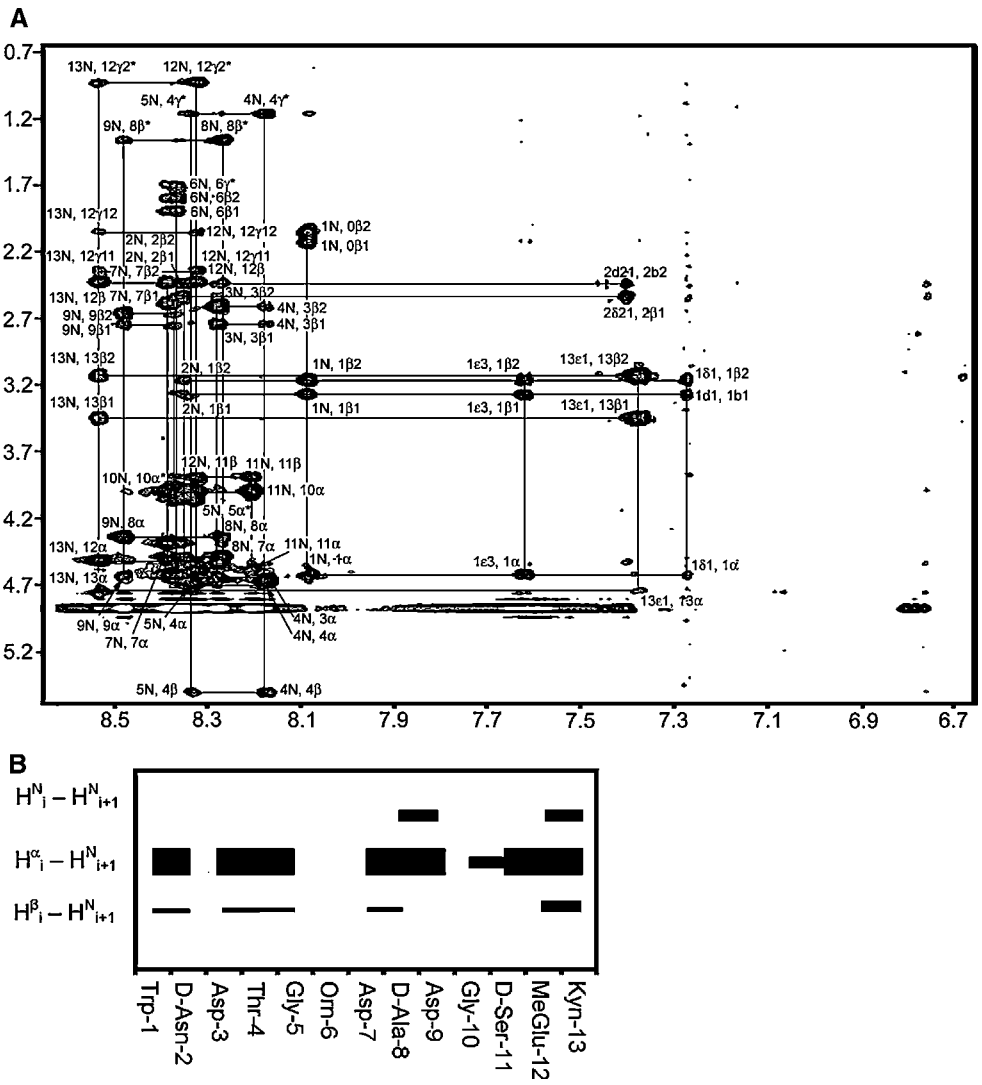

Fig. 2 **a** NOESY spectra for Mg^{2+}-substituted daptomycin recorded at 18°C at a mixing time of 150 ms (see text for further experimental details). NOE crosspeaks between the backbone amide protons, α-protons, and sidechain protons are labeled. The residue number 0 refers to the *n*-decanoyl fatty acid chain on the N terminus. **b** Summary of the NOE-derived distance restraints used to generate the Mg^{2+}-substituted structures of daptomycin. The thickness of the bars corresponds to the strength of the NOE restraints, which were grouped into strong, medium, and weak, with upper bounds up to 3.0, 4.0, and 5.0 Å, respectively. Distance restraints to the *n*-decanoyl moiety, to H's which were not stereospecifically assigned e.g. contacts between $H_i^{\beta 1}$–H_{i+1}^N and $H_i^{\beta 2}$–H_{i+1}^N are represented by a single bar, and to more distant protons are not included in **b**

Table 3 Statistical analysis for the NMR-Derived structure of Mg^{2+}-substituted daptomycin

No. of NOE restraints	62
Interresidue	39
Intraresidue	23
No. of NOE restraint violations >0.1 Å[a]	47 ± 2
Average highest NOE restraint violation (Å)[a]	0.19 ± 0.07

	Average pairwise RMSD to the mean (Å)[a, b]	
Residue No.	Backbone	Heavy atom
1–13	1.57 ± 0.06	2.92 ± 0.08
4–13	1.30 ± 0.05	2.38 ± 0.07
3–8	1.11 ± 0.06	2.01 ± 0.10

Structures were calculated using the DGII program in Insight II v. 97.2 (Accelrys, San Diego, CA)

[a] Expressed as mean ± standard deviation of 15 accepted of the 40 calculated

[b] Calculated using MOLMOL 2K.2

table for comparison purposes. In order to effectively bind Ca^{2+} around the proposed site, additional constraints were employed between Ca^{2+} and atoms assumed to be involved in the binding process. In all cases, at least four oxygen atoms were involved in these additional constraints of each model to reflect the fact that Ca^{2+} normally requires four or more coordination sites to form a complex. The Ca^{2+}-O distance was set to be 0.25 nm in all cases. Binding to the Asp side chains was modeled by a single distance constraint of length 0.28 nm to the Cγ atoms. This was done so that Cγ, rather than the two oxygen atoms on the aspartate side chains bore the distance constraint, thereby allowing more degrees of freedom, such as rotations, to be probed.

To quantify the extent of deviation of a simulated structure from experimental NOE derived distances (Jung et al. 2004), an average relative NOE violation was calculated, as described in the "Methods and Supplemental Material sections". Violations were calculated with respect to the NOE distance restraints obtained experimentally for

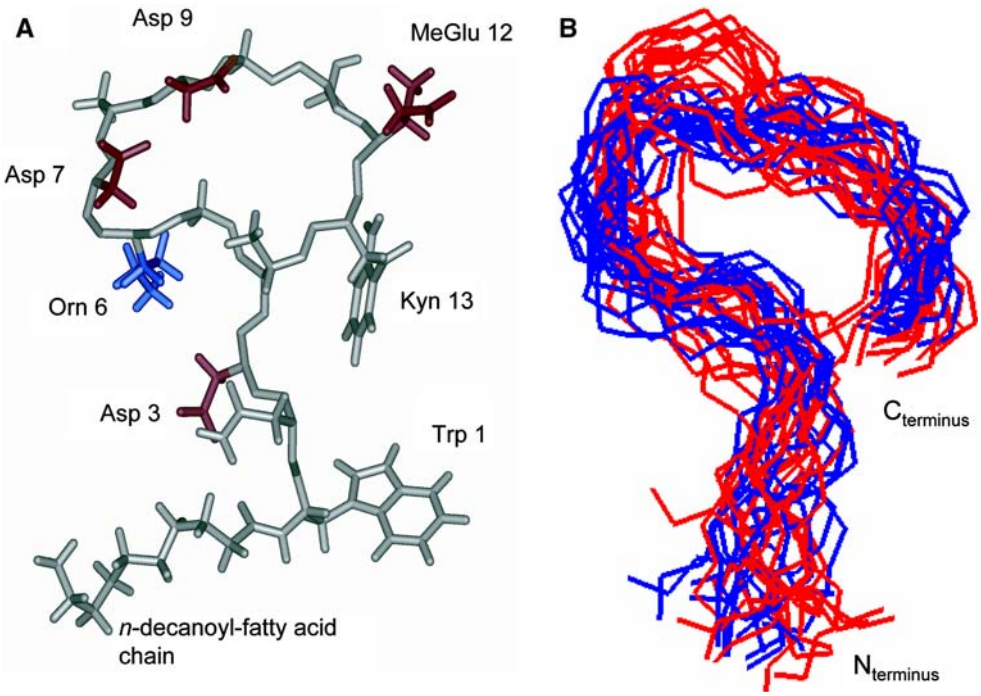

Fig. 3 Structures of daptomycin in the presence of 2.5 molar equivalents of Mg^{2+}: **a** stick model of the Mg^{2+}-conjugated daptomycin closest to the average, with the negatively charged residues colored *red* and the positively charged residue colored *blue*; **b** superposition of the backbone representations of the 15 accepted structures for Mg^{2+}-conjugated daptomycin (*blue*) and 15 previously accepted structures for apo-daptomycin (*red*) (Jung et al. 2004). The amino acid sequence of daptomycin is as follows: *n*-decanoyl-Trp-D-Asn-Asp-Thr-Gly-Orn-Asp-D-Ala-Gly-D-Ser-(2S, 3R) 3-MeGlu-Kyn. For clarity, only selected residues were labelled in **a**. The figure in **a** was prepared using Insight II v.97.2 (Accelrys Inc., San Diego, CA) and in **b** using MOLMOL 2K.2 (Koradi et al. 1996)

Ca^{2+}-bound daptomycin, as well as the apo-form. The resulting average violations are shown in Fig. 4 for all models (instantaneous values not shown, see Fig. 4 caption). It is evident that, for all models tested, no single model agreed markedly better than any other with the experimental NOE data for both the calcium bound structure and the apo-form, as observed by the more or less constant height of the grey and white bars, respectively. This signifies that no single model, allowed to undertake dynamics with calcium constrained at a given position, fulfilled the NOE constraints fully. More importantly, if one compares the models to the original conformation determined experimentally (i.e. for i17, we calculate $\overline{V}_{rel}$ with respect to structure 17 in 1T5N), shown by the solid bars in Fig. 4, all the models with a calcium restraint present have significantly higher violations. Overall, it can be concluded that none of the Ca^{2+}-bound daptomycin models tested here are consistent with the NOE restraints for 1T5N reported in Jung et al. (2004). The reasons for this inconsistency may either be that the NOE restraints are incorrect, that the Ca^{2+} binding sites tested are wrong, or both.

In light of these observations, we compared the NOE data of the apo- and the Ca^{2+}-bound forms of daptomycin (Jung et al. 2004) and the corresponding proposed large difference in backbone ring conformation between these two models. In the Ca^{2+}-bound case, the backbone ring is severely constrained by distance restraints between Asp 3 and Ala 8 located at approximately diametrically opposed sides of the ring (Fig. 5). As these restraints are not observed in the apo form, the proposed ring structure is much more circular in this case. Here, based on the fact that we now know that daptomycin oligomerizes in the presence of Ca^{2+}, we hypothesize that these additional NOE restraints between residues 3 and 8 are intermolecular and should therefore not be included when refining the structure of an individual molecule, which is determined by intramolecular restraints. Two refinement simulations, each 30 ns in length, were performed using the thus modified Ca^{2+}-bound NOE restraints, starting from the 1T5M and 1T5N consensus models. A cluster analysis (see Supplemental Material for details) was performed in order to determine the dominant conformer of the simulations, shown in Fig. 5c, d for the starting 1T5M and 1T5N models, respectively. Overall, the removal of the three restraints resulted in more extended ring structures (Fig. 5c, d, respectively), much more like the apo-form (Fig. 5a). The relative NOE violations versus the original

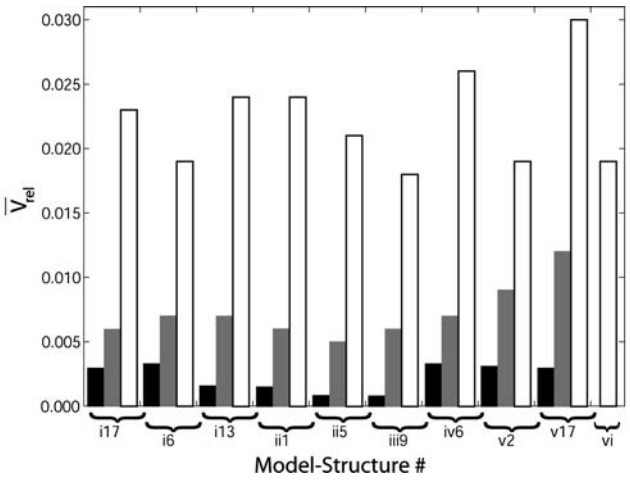

Fig. 4 Histogram of the calculated average relative NOE violations for the different calcium binding modes tested here (Table 1). The *X*-axis is the binding mode/NMR structure used as a starting configuration in the simulation. The solid *black bars* represent the NOE violations calculated with respect to the original NMR structure. The *grey bars* represent NOE violations compared to experimentally derived NOE restraints for the calcium bound daptomycin. The *white bars* represent NOE violations compared to experimentally derived NOE restraints for the apo-form of daptomycin. Values obtained from simulations performed using instantaneous refinement were generally only slightly different from the time-averaged results. Therefore, for clarity, they are not shown here

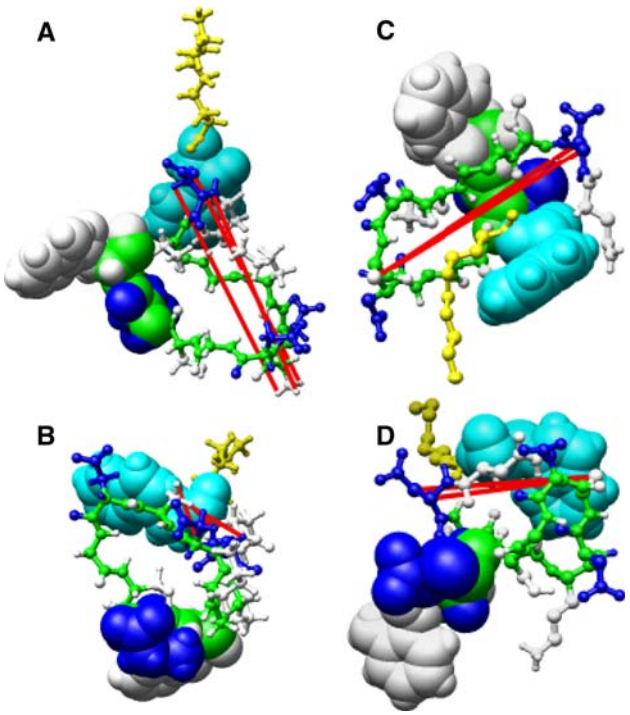

Fig. 5 Representative daptomycin structures, with the three distances between the ^{1}H's in Asp3 and Ala8 highlighted by *red* lines. **a** Apo-form (1T5M, consensus model). **b** Calcium-bound form (1T5N, consensus model). **c** New calcium-bound structure starting from the apo-form in **a**, obtained from a refinement where three NOEs between Asp3 and Ala8 are reclassified as being intermolecular. **d** New calcium-bound structure starting from the calcium-bound form in **b**, obtained from a refinement where three NOEs between Asp3 and Ala8 are reclassified as being intermolecular. The residues shown in CPK are those, which are significantly broadened/shifted in the ^{13}C NMR Ca^{2+} titration data, with Trp1 shown in *cyan*, MeGlu12 shown in *blue*, and Kyn13 shown in *white*. The residues shown in ball-and-stick representation in *blue* are the Asp side-chains. The cyclic backbone is shown in *green* and finally, the *n*-decanoyl fatty acid chain is shown in *yellow*. Both conformations in **c** and **d** largely fulfill the NOE restraints (see Table 4), yet they are significantly different. This suggests that a unique structure cannot be defined given the inherent flexibility of the lipopeptide

and the modified Ca^{2+}-bound datasets as well as versus the apo-form dataset were calculated (Table 4). It can be seen that, in these simulations using the modified Ca^{2+}-bound dataset as restraints, the violations calculated relative to the apo form dataset (0.017 and 0.024) are considerably smaller than versus the original Ca^{2+}-bound dataset (0.055 and 0.041), indicating that the structures sampled here are more representative of the apo form. Furthermore, of the two simulations, the one starting from the 1T5M apo structure has lower violations relative to the apo-form dataset (0.017) than the one starting from the proposed Ca^{2+}-bound structure 1T5N (0.024). Taken together, these simulations suggest that the Ca^{2+}-bound structure of daptomycin may not after all differ significantly from the apo-form, under the assumption that the additional NOE restraints in the Ca^{2+}-bound case are due to intermolecular contacts that occur upon oligomerization.

Ca^{2+} titration and possible oligomer arrangement

In order to further characterize which residues are important for either calcium binding or oligomer formation, we examined the effect of adding increased amounts of Ca^{2+} to a daptomycin solution in the range of 0–1.4 equivalents by one-dimensional ^{13}C NMR (Fig. 6). Previous studies (Ball et al. 2004; Jung et al. 2004; Rotondi and Gierasch 2005) indicated that addition of calcium to daptomycin led to a broadening of all the ^{1}H lines observed in the NMR spectra. This change in linewidth has a sigmoidal dependence on the amount of calcium added, suggesting cooperative binding, and levels off at a 1:1 molar ratio of calcium to daptomycin. As the chemical shift range for carbon is much larger than for ^{1}H, we chose to look at ^{13}C NMR here to see whether large changes with increasing calcium concentration (Colpitts et al. 1995; Vishwanath and Easwaran 1981) could be observed. The spectra for which some of the resonances have been assigned (see "Methods") are shown in Fig. 6 and illustrate how these changes manifest themselves. All the lines broadened significantly upon addition of calcium and showed a sigmoidal dependence, as seen for Asn2 CO, MeGlu12 CO

Table 4 Calculated relative NOE violations for the conformations sampled in the 30 ns refinement simulations starting from the apo- (1T5M) and Ca^{2+}-conjugated (1T5N) consensus models, when different NOE restraints are considered (see text)

	Starting from	
NOE restraints	1T5M	1T5N
Ca^{2+}-bound form (all NOE restraints)	0.055	0.041
Ca^{2+}-bound form (with 3 Asp3/Ala8 restraints removed)	0.019	0.020
Apo-form (all NOE restraints)	0.017	0.024

and Orn6 Cδ (not shown, resonates at 42.10 ppm), for instance, and most of the other lines. This broadening was accompanied by very slight changes in chemical shift (on the order of 0.1–0.2 ppm). For four lines, however, the dependence on the linewidth was more complex, namely for the sidechain carbonyl carbon of Kyn13, Cα of Kyn13 (not shown), Cδ2 carbon of Trp1, and Cγ of MeGlu12 (not shown). In this case, the changes in chemical shift (ca. 0.5–0.6 ppm) (and/or linewidth) were comparatively larger, but still very small when compared to chemical shift changes of peptides which change conformation significantly upon binding divalent ions such as Ca^{2+} (i.e. on the order of 2–8 ppm) (Vishwanath and Easwaran 1981). From the small chemical shift perturbations observed, it would appear that the addition of calcium had only a small effect on conformation, supporting the reinterpretation of the NOESY data discussed above. It is important to note, however, that caution should be exercised when using the chemical shift alone as a diagnostic of structural changes in small peptides (Daura et al. 1997).

Discussion

Many studies over the years (Laganas et al. 2003; Lakey et al. 1989; Lakey and Ptak 1988; Silverman et al. 2003) have shown the importance of calcium for daptomycin activity. In this contribution, we have shown that the addition of the divalent cations Ca^{2+} and Mg^{2+} to a daptomycin solution leads to the formation of micelles, thus confirming a previous suggestion by Rotondi and Gierasch (2005). It is noteworthy that micelle formation has also been suggested for tsushimycin (Bunkoczi et al. 2005), suggesting a possible common mode of action. In the case of daptomycin in the presence of calcium, aggregation occurred in the presence of one molar equivalent, while for Mg^{2+} a much larger fraction of ion (2.5 times) is needed. This indicates that the interaction between magnesium ion and daptomycin is weaker than that between Ca^{2+} and daptomycin. In fact, substituting Ca^{2+} with various divalent cations resulted in a minimum 32-fold increase in the MIC of daptomycin. Moreover, substituting Ca^{2+} with Mg^{2+} resulted in very few changes in the two-dimensional

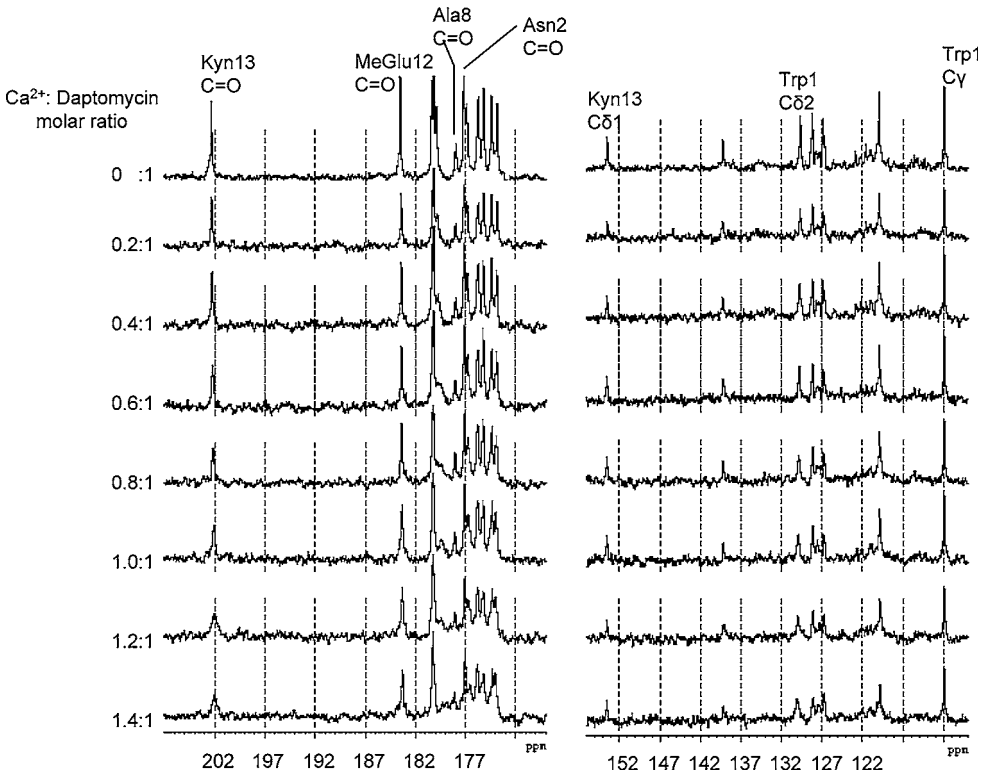

Fig. 6 One-dimensional ^{13}C NMR spectrum of the carbonyl region of daptomycin as a function of increasing amounts of calcium (see text for experimental details). Most lines are broadened in a sigmoidal concentration dependence, with sidechain carbonyl carbon of Kyn13, Cα of Kyn13, Cδ2 carbon of Trp1, and Cγ of MeGlu12 being most strongly affected

^{1}H NMR spectra in terms of line-broadening and the appearance of new NOEs, as compared to the corresponding spectra for the apo-form of daptomycin. Given that Mg^{2+} is much smaller than Ca^{2+}, it is often a poor substitute for calcium in calcium-binding peptides and proteins. For example, annexin II possesses two types of Ca^{2+} binding sites and it has been shown that occupation of only one of the two Ca^{2+}-binding sites is required for the intracellular association of annexin II with the submembraneous cytoskeleton in HeLa cells (Jost et al. 1994). However substituting Ca^{2+} with other divalent metal ions has a negative effect on the annexin-mediated aggregation of asolectin liposomes (Jost et al. 1994).

Despite the difference in binding affinity, it would appear that one of the roles of divalent cations such as Ca^{2+} and Mg^{2+} is to promote the formation of micellar structures in solution. Given that daptomycin has a large hydrophobic tail, micellar structures would not be surprising. As demonstrated here, the oligomerization process may not necessarily be accompanied by a structural change in daptomycin itself. In the case where magnesium is added, no new NOEs were found and the structure of daptomycin in the presence of Mg^{2+} was much the same as the one reported for the apo-form (Jung et al. 2004). Similarly, if one reinterprets the NOESY spectra of calcium-conjugated daptomycin such that some of the new NOEs observed upon addition of Ca^{2+} arise from intermolecular contacts, then the structure of daptomycin is in this case also extended, as in the apo-form. This suggests that the structural transition, proposed by Jung et al. to occur upon Ca^{2+} binding to enhance the amphipathicity of daptomycin and result in insertion into the membrane, may not occur. Instead, divalent cation binding is proposed here to serve to form micelles, which are the vehicles that deliver high local concentrations of daptomycin to the bacterial membrane (Straus and Hancock 2006). Another, not necessarily exclusive, possibility is that micelle formation simply reflects a sharp transition of daptomycin to "detergent-like" behavior and consequent increased membrane-disruptive potential. Given that calcium ions interact more strongly with negatively charged lipid headgroups than do magnesium ions (Garidel and Blume 2005), the difference in the activity of daptomycin in the presence of these divalent cations may then account for how strongly daptomycin interacts with PC/PG membranes. In other words, Ca^{2+} forms a better bridge between the negatively charged daptomycin and bacterial membranes than does Mg^{2+}. Consistent with this view, Mg^{2+} was unable to promote an alteration in CD spectrum in the presence of anionic lipids, or calcein release from PC:PG liposomes (Jung and Hancock, unpublished).

It is interesting to note that there are considerable differences in the proposed three structures of apo daptomycin. As already mentioned in the introduction, the backbone Cα RMSDs between the 1T5M consensus structure and 1XT7 (3.2 Å) and the Rotondi and Gierasch structures (>4 Å, for the family of 6 structures that emerged from their RMSD analysis (Rotondi and Gierasch 2005)) are not negligible. The differences are larger if the lipid tail and side chains are taken into account. We suggest that this wide spread of proposed structures reflects the very high mobility of daptomycin in the apo form. Furthermore, the reinterpretation of the three cross peaks as being intermolecular in the Ca^{2+}-bound form has another important consequence in that the flexibility of daptomycin is not reduced with respect to the apo form in this model (as evidenced by the two structures in Fig. 5c, d, which both satisfy the NOE restraints). As a consequence, it will be very difficult to sample all relevant configurations during the course of a simulation. This in turn means that the result of any refinement procedure using MD will be biased by choices made in the refinement protocol, notably by the choice of (a) the starting structure and (b) the form of restraint (instantaneous or time-averaged). This phenomenon is apparent from Table 4: refinement starting from very different daptomycin structures, 1T5N and 1T5M, produced NOE violations versus the modified Ca^{2+}-bound NOE restraints that are very similar (0.019 and 0.020). A subsequent cluster analysis (Supplemental) shows, however, that the phase space sampled in these simulations hardly overlaps at all (less than 1%, data not shown), indicating that in any one simulation, many relevant data points are not sampled.

Finally, given the line-broadening in the ^{13}C NMR spectra and the results from the molecular dynamics simulations, we propose that residues Trp1, MeGlu12, and Kyn13 are at the intermolecular interface and that the calcium ion serves to neutralize the negative charge between the daptomycin molecules in the micelle. One possible arrangement of daptomycin that would take this evidence into account would be to pack the daptomycin molecules together such that a favorable π-stacking interaction can occur between the aromatic rings of Trp1 on one molecule and Kyn13 on another. Calcium ions would then be at the interface between the daptomycin molecules to minimize electrostatic repulsions between negatively charged residues, which need to come into contact to form the multimer. Alternatively, the calcium ions may be associating with the daptomycin micelle surface, in a manner analogous to the interaction of Ca^{2+} with POPC/POPG membranes, where the calcium ions move freely on the bilayer surface (Macdonald and Seelig 1987; Seelig 1990), driven by the electrostatics at the membrane surface (Watts and Poile 1986). Overall, this daptomycin/calcium arrangement would result in the lipid tails, which are very flexible, packing together towards the interior of a micellar structure. The recent results reported by Grunewald et al.

(2004) that the residues MeGlu12 and Kyn13 are crucial for activity combined with our findings suggest that micelle formation may be an important step in the mode of action of daptomycin. In Grunewald et al. (2004), MeGlu12 was replaced by Gln, resulting in an increase in MIC of a factor of 10 relative to native daptomycin. Likewise, the MIC increased by a factor of 4–33 when Kyn13 was replaced, depending on the reports (Grunewald et al. 2004; Nguyen et al. 2006). This indicates that interactions needed to hold the multimer together, such as for example a hydrogen bond between the sidechain carbonyl carbon of Kyn13 and the sidechain NH group in Trp1 or an electrostatic interaction between the carboxyl group in MeGlu12 and Ca^{2+}, might have a direct bearing on activity.

In conclusion, the data presented here illustrate the role of divalent cations in lipopeptide function. We suggest that divalent cations such as Ca^{2+} or Mg^{2+} serve to mask the negatively charged residues in anionic lipopeptides such as daptomycin, thereby enabling the antibiotic to interact and perturb bacterial membranes in a detergent-like manner, analogous to what has been suggested for cationic antimicrobial peptides (Bechinger 1999; Bechinger and Lohner 2006). The stronger interaction of calcium over magnesium with daptomycin and lipids makes it a more effective shield. In effect, therefore, lipopeptides such as daptomycin appear to behave like cationic antimicrobial peptides.

Acknowledgments The authors would like to thank Jared Silverman for useful discussions. The authors would also like to acknowledge funding by the Canada Foundation for Innovation (CFI) for the C-HORSE computer centre. The authors gratefully acknowledge the support of NSERC through a Discovery Grant and a University Faculty Award and UBC to SKS, as well as funding from the Canadian Institutes of Health Research and Cubist Pharmaceuticals Inc to REWH. REWH held a Canadian Research Chair. JDL acknowledges funding from the NIH (GM60610). Molecular graphics images were produced using the UCSF Chimera package from the Computer Graphics Laboratory, University of California, San Francisco (supported by NIH P41 RR-01081).

References

Amsterdam D (1996) Susceptibility testing of antimicrobials in liquid media. In: Loman V (ed) Antibiotics in laboratory medicine. Williams and Wilkins, Baltimore, MD, pp 52–111

Ball LJ, Goult CM, Donarski JA, Micklefield J, Ramesh V (2004) NMR structure determination and calcium binding effects of lipopeptide antibiotic daptomycin. Org Biomol Chem 2:1872–1878

Bechinger B (1999) The structure, dynamics and orientation of antimicrobial peptides in membranes by multidimensional solid-state NMR spectroscopy. Biochim Biophys Acta 1462:157–183

Bechinger B, Lohner K (2006) Detergent-like actions of linear amphipathic cationic antimicrobial peptides. Biochim Biophys Acta 1758:1529–1539

Berendsen HJC, Postma JPM, van Gunsteren WF, Hermans J (1981) Interaction models for water in relation to protein hydration. In: Pullman B (ed) Intermolecular forces. Reidel, Dordrecht, pp 331–342

Berendsen HJC, Postma JPM, van Gunsteren WF, Dinola A, Haak JR (1984) Molecular-dynamics with coupling to an external bath. J Chem Phys 81:3684–3690

Boaretti M, Canepari P, Lleo MD, Satta G (1993) The activity of daptomycin on enterococcus-faecium protoplasts—indirect evidence supporting a novel mode of action on lipoteichoic acid synthesis. J Antimicrob Chemother 31:227–235

Braunschweiler L, Ernst RR (1983) Coherence transfer by isotropic mixing: application to proton correlation spectroscopy. J Magn Reson 53:521–528

Bunkoczi G, Vertesy L, Sheldrick GM (2005) Structure of the lipopeptide antibiotic tsushimycin. Acta Crystallogr D Biol Crystallogr 61:1160–1164

Chattopadhyaya R, Meador WE, Means AR, Quiocho FA (1992) Calmodulin structure refined at 1.7 angstrom resolution. J Mol Biol 228:1177–1192

Chazin WJ (1995) Releasing the calcium trigger. Nat Struct Biol 2:707–710

Colpitts TL, Prorok M, Castellino FJ (1995) Binding of calcium to individual gamma-carboxyglutamic acid residues of human protein C. Biochemistry 34:2424–2430

Daura X, van Gunsteren WF, Rigo D, Jaun B, Seebach D (1997) Studying the stability of a helical beta-heptapeptide by molecular dynamics simulations. Chem Eur J 3:1410–1417

Delaglio F, Grzesiek S, Vuister GW, Zhu G, Pfeifer J, Bax A (1995) NMRPipe: a multidimensional spectral processing system based on UNIX pipes J. Biomol NMR 6: 227–293

Eliopoulos GM, Willey S, Reiszner E, Spitzer PG, Caputo G, Moellering RCJ (1986) In vitro and in vivo activity of LY 146032, a new cyclic lipopeptide antibiotic. Antimicrob Agents Chemother 30:532–535

Fass RJ, Helsel VL (1986) Invitro activity of LY146032 against Staphylococci, Streptococci, and Enterococci. Antimicrob Agents Chemother 30:781–784

Garidel P, Blume A (2005) 1,2-Dimyristoyl-sn-glycero-3-phosphoglycerol (DMPG) monolayers: influence of temperature, pH, ionic strength and binding of alkaline earth cations. Chem Phys Lipids 38: 50–59

Grunewald J, Sieber SA, Mahlert C, Linne U, Marahiel MA (2004) Synthesis and derivatization of daptomycin: A chemoenzymatic route to acidic lipopeptide antibiotics. J Am Chem Soc 126:17025–17031

Jeener J, Meier BH, Bachmann P, Ernst RR (1979) Investigation of exchange processes by two-dimensional NMR spectroscopy. J Chem Phys 71:4546–4553

Johnson B, Blevins RA (1994) NMRView: a computer program for the visualization and analysis for NMR data. J Biomol NMR 4:603–614

Jones RN, Barry AL (1987) Antimicrobial activity and spectrum of LY146032, a lipopeptide antibiotic, including susceptibility testing recommendations. Antimicrob Agents Chemother 31:625–629

Jost M, Weber K, Gerke V (1994) Annexin II contains two types of Ca(2+)-binding sites. Biochem J 298(Pt 3):553–559

Jung D, Rozek A, Okon M, Hancock REW (2004) Structural transitions as determinants of the action of the calcium-dependent antibiotic daptomycin. Chem Biol 11:949–957

Kopp F, Grunewald J, Mahlert C, Marahiel MA (2006) Chemoenzymatic design of acidic lipopeptide hybrids: new insights into the structure-activity relationship of daptomycin and A54145. Biochemistry 45:10474–10481

Koradi R, Billeter M, Wüthrich K (1996) MOLMOL: a program for display and analysis of macromolecular structures. J Mol Graph 14:51–55

Laganas V, Alder J, Silverman JA (2003) In vitro bactericidal activities of daptomycin against *Staphylococcus aureus* and *Enterococcus faecalis* are not mediated by inhibition of lipoteichoic acid biosynthesis. Antimicrob Agents Chemother 47:2682–2684

Lakey JH, Maget-Dana R, Ptak M (1989) The lipopeptide antibiotic A21978C has a specific interaction with DMPC only in the presence of calcium ions. Biochim Biophys Acta 985:60–66

Lakey JH, Ptak M (1988) Fluorescence indicates a calcium-dependent interaction between the lipopeptide antibiotic Ly146032 and phospholipid-membranes. Biochemistry 27:4639–4645

Macdonald PM, Seelig J (1987) Calcium binding to mixed phosphatidylglycerol-phosphatidylcholine bilayers as studied by deuterium nuclear magnetic resonance. Biochemistry 26:1231–1240

Marsden BJ, Shaw GS, Sykes BD (1990) Calcium-binding proteins—elucidating the contributions to calcium affinity from an analysis of species variants and peptide-fragments. Biochem Cell Biol 68:587–601

Massiot D, Fayon F, Capron M, King I, Le Calvé S, Alonso B, Durand J-O, Bujoli B, Gan Z, Hoatson G (2002) Modelling one- and two-dimensional solid state NMR spectra. Magn Reson Chem 40:70–76

Nguyen KT, Ritz D, Gu JQ, Alexander D, Chu M, Miao V, Brian P, Baltz RH (2006) Combinatorial biosynthesis of novel antibiotics related to daptomycin. Proc Natl Acad Sci USA 103:17462–17467

Rance M, Sorensen O, Bodenhausen G, Wagner G, Ernst RR, Wüthrich K (1983) Improved spectral resolution in COSY 1H NMR spectra of proteins via double quantum filtering. Biochem Biophys Res Commun 117:479–485

Rotondi KS, Gierasch LM (2005) A well-defined amphipathic conformation for the calcium-free cyclic lipopeptide antibiotic, daptomycin, in aqueous solution. Biopolymers 80:374–385

Rozek A, Friedrich CL, Hancock RE (2000) Structure of the bovine antimicrobial peptide indolicidin bound to dodecylphosphocholine and sodium dodecyl sulfate micelles. Biochemistry 39:15765–15774

Ryckaert JP, Ciccotti G, Berendsen HJC (1977) Numerical-integration of Cartesian equations of motion of a system with constraints—molecular-dynamics of *N*-Alkanes. J Comput Phys 23:327–341

Scott WRP, Hunenberger PH, Tironi IG, Mark AE, Billeter SR, Fennen J, Torda AE, Huber T, Kruger P, van Gunsteren WF (1999) The GROMOS biomolecular simulation program package. J Phys Chem A 103:3596–3607

Seelig J (1990) Interaction of phospholipids with Ca^{2+} ions. On the role of the phospholipid head groups. Cell Biol Int Rep 14:353–360

Silverman JA, Oliver N, Andrew T, Li T (2001) Resistance studies with daptomycin. Antimicrob Agents Chemother 45:1799–1802

Silverman JA, Perlmutter NG, Shapiro HM (2003) Correlation of daptomycin bactericidal activity and membrane depolarization in *Staphylococcus aureus*. Antimicrobl Agents Chemother 47:2538–2544

Straus SK, Hancock RE (2006) Mode of action of the new antibiotic for Gram-positive pathogens daptomycin: comparison with cationic antimicrobial peptides and lipopeptides. Biochim Biophys Acta 1758:1215–1223

Streit JM, Steenbergen JN, Thorne GM, Alder J, Jones RN (2005) Daptomycin tested against 915 bloodstream isolates of viridans group streptococci (eight species) and *Streptococcus bovis*. J Antimicrob Chemother 55:574–578

Tally FP, DeBruin MF (2000) Development of daptomycin for Gram-positive infections. J Antimicrob Chemother 46:523–526

Tironi IG, Sperb R, Smith PE, van Gunsteren WF (1995) A generalized reaction field method for molecular-dynamics simulations. J Chem Phys 102:5451–5459

Torda AE, van Gunsteren WF (1991) The refinement of NMR structures by molecular-dynamics simulation. Comput Phys Commun 62:289–296

van Gunsteren WF, Billeter SR, Eising AA, Huenenberger PH, Krueger P, Mark AE, Scott WRP, Tironi IG (1996) Biomolecular simulation: the GROMOS96 manual and user guide. VdF: Hochschulverlag AG an der ETH Zurich BIOMOS b.v., Zurich, Groningen

Vishwanath CK, Easwaran KR (1981) Hydrogen-1 and carbon-13 magnetic resonance studies of nonactin-calcium complex. Biochemistry 20:2018–2023

Watts A, Poile TW (1986) Direct determination by 2H-NMR of the ionization state of phospholipids and of a local anaesthetic at the membrane surface. Biochim Biophys Acta 861:368–372

Wüthrich K (1986) NMR of proteins and nucleic acids/Kurt Wüthrich. Wiley, New York